DOI: 10.1002/ejic.200800506

2-Thiopheneacetato-Based One-Dimensional Coordination Polymer of Tb^{3+}: Enhancement of Terbium-Centered Luminescence in the Presence of Bidentate Nitrogen Donor Ligands

Shyni Raphael,[a] M. L. P. Reddy,*[a] Alan H. Cowley,[b] and Michael Findlater[b]

Keywords: Enhanced terbium luminescence / 2-Thiopheneacetic acid / Bidentate nitrogen donors / 1D Coordination polymer

Four new lanthanide(III) complexes of 2-thiopheneacetic acid (HTPAC), $[Tb(TPAC)_3{\cdot}H_2O]_n$ (**1**), $[Gd(TPAC)_3{\cdot}H_2O]_n$ (**2**), $[Tb(TPAC)_3(phen)]_2$ (**3**) and $[Tb(TPAC)_3(bath)]_2$ (**4**) (phen = 1,10-phenanthroline; bath = bathophenanthroline) have been synthesized and characterized by various spectroscopic techniques. The X-ray structure of **1** reveals that each Tb^{3+} ion is connected to two neighboring ions by six thiopheneacetic acid ligands via the carboxylate groups to form an infinite one-dimensional polymer. The unit cell contains only one independent crystallographic site for the Tb ions. The carboxylate groups of the six molecules of the thiopheneacetate ligands are coordinated in both bidentate bridging and tridentate chelate-bridging modes. Each Tb^{3+} ion is coordinated by nine oxygen atoms in an overall distorted tricapped trigonal-prismatic geometry. Eight of the oxygen atoms are furnished by the carboxylate moieties, and the remaining oxygen atom is provided by the water molecule. The photophysical properties of these complexes in the solid state at room temperature have been investigated. The quantum yields of **3** (4.43 ± 0.44 %) and **4** (9.06 ± 0.90 %) were found to be significantly enhanced by the presence of the bidentate nitrogen donor ligands in comparison with that of **1** (0.07 ± 0.01 %) due to effective energy transfer from the secondary ligands.

Introduction

The fascinating optical properties of lanthanide ions have promoted the use of such complexes in a wide variety of technological applications ranging from biomedical analysis to materials science.[1–6] Furthermore, lanthanide ions exhibit characteristically sharp emissions in the visible and near-infrared regions, long luminescence lifetimes, and large Stokes shifts, which renders them very attractive candidates for the development of optical devices.[7–9] However, the usual impediment to the use of such lanthanide ion systems is that the direct absorption of the f–f excited states is very inefficient. In the case of the lanthanide ions, the f–f transitions are parity forbidden which results in very low absorption coefficients. In order to overcome this drawback, suitable chromophores have been employed as antennas or sensitizers that have the capability of transferring energy indirectly to the lanthanide ions.[10] The photophysical properties of Ln^{3+} ions therefore depend critically on their ligand environments. In particular, it is important to protect the lanthanide metal center from solvent molecules which can quench the desired emissions. In this context, numerous ligands have been shown to serve as the "antenna". The list includes β-diketones,[9–12] and aromatic carboxylic acids.[13]

In the recent past, aromatic carboxylate coordination complexes possessing unique photophysical properties and intriguing structural features, have attracted considerable attention.[14] In the case of lanthanide monocarboxylate complexes, the carboxylate groups can bind to the lanthanide ion in monodentate, chelating, bridging, and bridging-chelating modes. As a consequence, such complexes can exhibit mononuclear, dinuclear, polymeric chain, or network structures. Generally speaking, the lanthanide complexes of monoacids form coordination polymers with bridging carboxylato groups. Examples include Eu^{3+} and Tb^{3+} nitrobenzoate complexes,[15] Ln^{3+} *p*-aminobenzoates,[16] Eu^{3+} 2,3-dimethoxybenzoates[17] and $Ce^{3+}/Sm^{3+}/Pr^{3+}$ 2-thiopheneacetate complexes.[18] On the other hand, the lanthanide complexes of a monoacid and 1,10-phenanthroline (phen) or 2,2′-bipyridine (2,2′-bpy) are typically dimeric and feature the carboxylato groups as bridging ligands, as exemplified by $[Eu_2(3,4\text{-DMBA})_6{\cdot}(phen)_2]$[19] (3,4-DMBA = 3,4-dimethylbenzoate) and $[Tb(2\text{-FBA})_3{\cdot}phen]_2$ (2-FBA = 2-fluorobenzoate).[20] The lanthanide carboxylates that involve 2,2′-bpy or phen ligands have particularly interesting structures. They also exhibit high stabilities and intense

[a] Chemical Sciences and Technology Division, National Institute for Interdisciplinary Science & Technology (NIIST), Thiruvananthapuram 695019, India
E-mail: mlpreddy@yahoo.co.uk
[b] Department of Chemistry and Biochemistry, The University of Texas at Austin,
1 University Station A5300, Austin, Texas 78712, USA
E-mail: cowley@mail.utexas.edu
Supporting information for this article is available on the WWW under http://www.eurjic.org or from the author.

fluorescence emissions. Bipyridines and phenanthrolines, can serve as co-chelating and co-sensitizing ligands, and, as such, circumvent solubility or volatility problems by forming new molecular geometries. Moreover, these types of ligand shield the immediate chemical environment of the metal ion from the ingress of water, which is known to diminish luminescence efficiencies.

It has been recognized that thiophene-derivatization in nitrobenzoic and isophthalic acids exhibited enhanced terbium-centered luminescence as compared to unsubstituted ligands.[21,22] A preliminary study by Malta and coworkers[23] demonstrated that thiopheneacetic acid (HTPAC) can be used as a potential sensitizer for lanthanide emissions. However, to the best of our knowledge, systematic investigations of the luminescent properties of terbium thiopheneacetate complexes in the presence of bidentate nitrogen donors and the structural characterization of such complexes by single-crystal X-ray diffraction have not been reported previously. This has prompted us to synthesize a series of terbium complexes featuring the thiopheneacetic acid ligand. Herein, we describe the syntheses, characterization and photophysical properties of three terbium thiopheneacetate complexes that also involve the coordination of bidentate nitrogen donors. The Tb^{3+} thiopheneacetate aqua complex was structurally characterized by single-crystal X-ray diffraction.

Results and Discussion

Characterization of Lanthanide Complexes

The elemental analysis and spectroscopic data for **1** and **2** indicate that Ln^{3+} ion has reacted with HTPAC in a metal-to-ligand mol ratio of 1:3. On the other hand, the microanalyses and FAB-MS studies of the compounds **3** and **4** revealed that Tb^{3+} ion has reacted with HTPAC in a metal-to-ligand mol ratio of 2:6 along with two molecules of the bidentate nitrogen ligand. Similar binuclear terbium carboxylate complexes, namely $[Tb(2\text{-}FBA)_3{\cdot}2,2'\text{-bpy}]_2$ and $[Tb(2\text{-}FBA)_3{\cdot}phen]_2$ (2-FBA = 2-fluorobenzoate), which also feature bidentate nitrogen donors have been reported elsewhere and characterized by means of single-crystal X-ray analysis.[20] In order to investigate the coordination modes of the HTPAC anion to the Ln^{3+} ion, the IR spectra of **1**–**4** were compared with that of the HTPAC ligand. The FT-IR spectrum of the HTPAC ligand evidences two intense bands at approximately 1450 and 1704 cm^{-1}, which are attributable to the symmetric υ_s(C=O) and *anti*-symmetric υ_{as}(C=O) vibration modes, respectively. In the cases of the IR spectra of **1**–**4**, both of these C=O vibrational modes are shifted to lower wave numbers and split into two peaks (1384, 1412 cm^{-1} and 1554, 1630 cm^{-1} in **1**; 1381, 1426 cm^{-1} and 1557, 1607 cm^{-1} in **2**; 1384, 1427 cm^{-1} and 1563, 1610 cm^{-1} in **3**; 1393, 1428 cm^{-1} and 1560, 1619 cm^{-1} in **4**), thus indicating coordination of the carbonyl oxygen to the Ln^{3+} cations. Furthermore, the IR spectra of these complexes exhibit a separation of the asymmetric and symmetric stretching vibrations [$\Delta\upsilon_{(C=O)} = \upsilon_{as} - \upsilon_s$] at approximately 240 and 142 cm^{-1} for **1**, 226 and 131 cm^{-1} for **2**, 226 and 136 cm^{-1} for **3**, 226 and 132 cm^{-1} for **4**, which implies coordination of the carboxylate group to the Ln^{3+} cation in a bidentate bridging and chelate mode in each case.[15,20,21] The IR spectra of **1** and **2** also exhibit a broad band at approximately 3451 and 3412 cm^{-1}, which is characteristic of an O–H stretching vibration υ(O–H), and thus suggestive of the presence of a coordinated water molecule in both complexes. Moreover, the red shifts observed for the C=N stretching frequencies of the nitrogen donors in the complexes **3** and **4** (1591 cm^{-1} in **3** and 1590 cm^{-1} in **4**) in comparison with those of the free ligands phen (1613 cm^{-1}) and bath (1608 cm^{-1}) imply coordination of these ligands to the Tb^{3+} cation in each case.

$[Tb(TPAC)_3{\cdot}H_2O]_n$ **1** $[Gd(TPAC)_3{\cdot}H_2O]_n$ **2**

$[Tb(TPAC)_3(phen)]_2$ **3** $[Tb(TPAC)_3(bath)]_2$ **4**

HTPAC = 2-thiopheneacetic acid
phen = 1,10-phenanthroline
bath = bathophenanthroline

The thermal decomposition behavior of the complexes **1**–**4** was investigated by means of TGA. Although no attempt has been made to identify the intermediate products formed during the thermal analysis, it is clear that the first step in the thermograms of complexes **1** and **2** (Figure S1, Supporting Information) corresponds to the loss of a coordinated water molecule in the temperature range 30–200 °C. Subsequent thermal decomposition takes place in two steps, and leaves a residue of approximately 60% of the initial mass for **1** and **2**, which corresponds to the formation of the corresponding lanthanide oxides. In contrast, complexes **3** and **4** are stable up to 260 and 275 °C, respectively. Both complexes undergo decomposition in two steps, and leave a residue that corresponds to terbium oxide (36% for **3** and 31% for **4**).

The X-ray powder diffraction patterns of complexes **1** and **2** are similar, indicating they are isostructural (Figure S2, Supporting Information). Similarly, from the XRD patterns of complexes **3** and **4** (Figure S2, Supporting Information), one can conclude that they are isostructural and crystalline.

X-ray Crystal Structure of $[Tb(TPAC)_3{\cdot}H_2O]_n$ (1)

The polymeric structure of complex **1** is illustrated in Figure 1 and Figure 2, and the details of the crystal data and data collection parameters are given in Table 1. A selection of pertinent bond lengths and bond angles is presented in Table 2. Compound **1** crystallizes in the orthorhombic space group *Pnma* with a = 7.835(10) Å, b = 19.378(10) Å, c = 13.539(10) Å, $\alpha = \beta = \gamma = 90°$ and V = 2055.6(3) $Å^3$. The unit cell features only one crystallographically independent site for the Tb cations and is labeled as Tb1. Interest-

ingly, other polymeric thiopheneacetate complexes of Ce^{3+}, Pr^{3+}, Nd^{3+}, Sm^{3+} and Eu^{3+} feature two independent Ln^{3+} complexes.[18] The X-ray structure of **1** reveals that each Tb^{3+} ion is connected to two neighboring cations by six carboxylate ligands to form an infinite one-dimensional chain along the *a* axis. Some of the HTPAC ligands are disordered, which has been treated in the normal fashion. The carboxylate groups of the six molecules of thiopheneacetate exhibit bidentate bridging and tridentate chelating-bridging modes, which corroborates well with the IR spectroscopic data. Two of the six carboxylate groups simultaneously bridge the two Tb^{3+} ions, while the other four carboxylate groups are chelated to two Tb^{3+} ions and simultaneously bridge two Tb^{3+} ions. Each Tb^{3+} is further surrounded by one H_2O molecule to form an overall nine-coordinate array around the metal. As shown in Figure 2, the coordination polyhedron of Tb1 is a distorted tricapped-trigonal prism. The intra-chain Tb1···Tb1^a distance of 4.048 Å, is smaller than the Ln···Ln distances reported for lanthanide thiopheneacetate complexes (4.274–4.311 Å for Ce^{3+}, 4.274–4.312 Å for Nd^{3+} and 4.159–4.261 Å for Eu^{3+}).[18,23] This trend can be explained on the basis of the lanthanide contraction. Since the Tb1^a–Tb1–Tb1^a angle is 150.86° it can be regarded as representing a linear chain along the *a* axis. The Tb–O (CO) bond lengths of the bidentate bridging carboxylate groups [2.292(10)–2.406(10) Å] are smaller than those of the tridentate chelating-bridging moieties [2.453(8)–2.502(7) Å]. On the other hand, the Tb–O distance of the coordinated water molecule

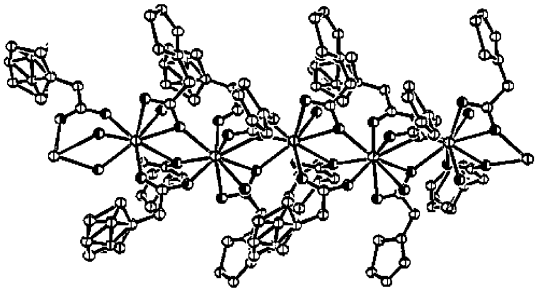

Figure 1. ORTEP diagram of complex **1**.

Table 1. Crystal data, collection, and structure refinement parameters for complex **1**.

Parameters	**1**
Empirical formula	$C_{18}H_{17}O_7S_3Tb$
Fw	600.42
Crystal system	orthorhombic
Space group	*Pnma*
Crystal size [mm]^3	$0.10 \times 0.15 \times 0.10$
Temperature	153(2)
a [Å]	7.835(10)
b [Å]	19.378(10)
c [Å]	13.539(10)
α [°]	90
β [°]	90
γ [°]	90
V [Å^3]	2055.6(3)
Z	4
$\rho_{calcd.}$ [g cm^{-3}]	1.940
μ [mm^{-1}]	3.783
F(000)	1176
R_1 [$I > 2\sigma(I)$]	0.0724
wR_2 [$I > 2\sigma(I)$]	0.1410
R_1 (all data)	0.1281
wR_2 (all data)	0.1552
GOF	1.24

Table 2. Selected bond lengths and bond angle of the complex **1**.

1	
Tb1–O3	2.292(10)
Tb1–O1^a	2.369(7)
Tb1–O1′	2.369(7)
Tb1–O4^a	2.406(10)
Tb1–O5	2.430(13)
Tb1–O2	2.453(8)
Tb1–O1	2.502(7)
Tb1–O2″	2.453(8)
Tb1–O1″	2.502(7)
Tb1–Tb1^a	4.048
O2–Tb1–O1	52.0(2)
O5–Tb1–O1	68.7(3)
O4^a–Tb1–O5	141.6(4)
O4^a–Tb1–O1″	79.0(2)
O2″–Tb1–O1″	52.0(2)
O1^a–Tb1–O2″	71.4(2)
O3–Tb1–O1′	75.9(3)
O3–Tb1–O1^a	75.9(3)
Tb1^a–Tb1–Tb1^a	150.86

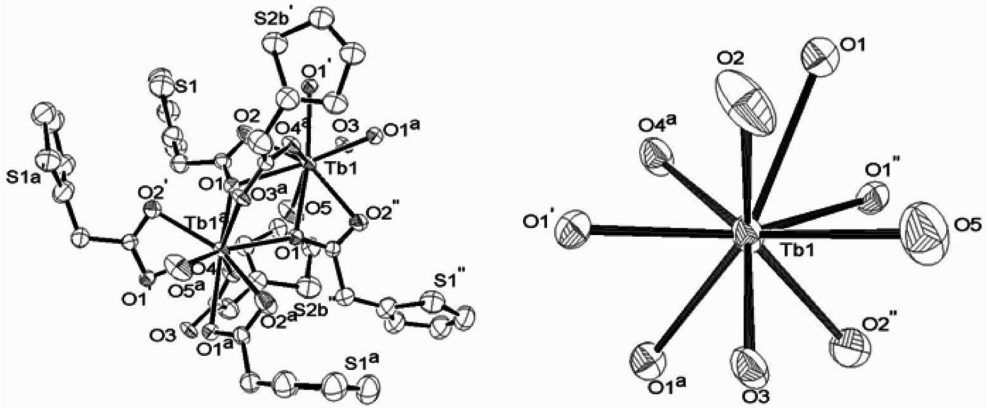

Figure 2. Coordination environment of the Tb^{3+} ions in this complex with atom-labeling scheme. All hydrogen atoms were omitted for clarity.

[2.430(13) Å] is shorter than those of the tridentate bridging ligand and longer than those of bidentate bridging ligand. Similar trends in bond lengths have been reported elsewhere[18,23] for polymeric thiopheneacetate complexes of Ce^{3+}, Pr^{3+}, Nd^{3+}, Sm^{3+} and Eu^{3+}.

UV/Vis Absorption Spectra

The UV/Vis absorption spectra of the free ligand HTPAC and the corresponding thiopheneacetate lanthanide complexes were measured in DMSO solution ($c = 2\times10^{-5}$ M), and are displayed in Figure 3. The absorption spectra of the neutral donors (phen, bath) are shown in Figure S3 of the Supporting Information. The absorption maxima for **1** (287 nm), **2** (287 nm), **3** (286 nm), and **4** (286 nm) which are attributable to singlet–singlet $^1\pi$–π^* absorptions of the aromatic rings, are slightly red-shifted with respect to that of the free ligand HTPAC (λ_{max} = 276 nm). The spectral contours for the complexes are similar to that of the free ligand, suggesting that the coordination of Ln^{3+} ion does not have a significant influence on the $^1\pi$–π^* transition. However, a small red-shift observed in the absorption band of each complex is a consequence of the enlargement of the conjugate structure of the ligand following coordination to the metal ion. The molar absorption coefficient values (ε) for **1** and **2** at λ_{max} are 1.64×10^4 and 1.72×10^4 L mol^{-1} cm^{-1}, respectively, and thus approximately three times larger than that of the free ligand HTPAC (6.44×10^3 at 276 nm), are indicative of the presence of three HTPAC ligands in both complexes. In contrast, the molar absorption coefficient values for complexes **3** and **4** (3.64×10^4 and 3.72×10^4 L mol^{-1} cm^{-1}), are six times larger than that for HTPAC, implying the presence of six thiopheneacetate ligands. Furthermore, the large molar absorption coefficient for HTPAC indicates that the carboxylic acid ligand has a strong ability to absorb light.

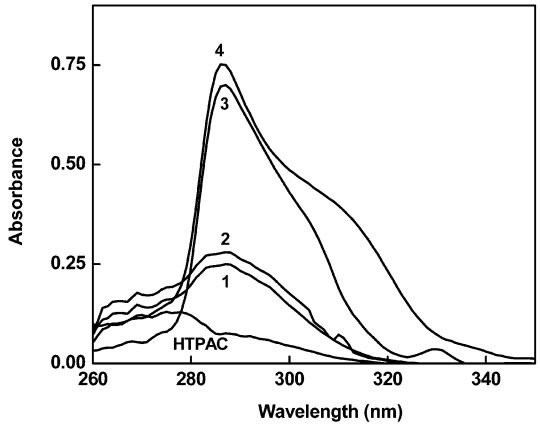

Figure 3. UV/Vis absorption spectra of ligand and complexes **1**–**4** in DMSO ($c = 2\times10^{-5}$ M).

PL Properties of Complexes 1–4

The photophysical properties of the HTPAC donor states in the Tb^{3+} complexes have been investigated on the basis of the phosphorescence spectrum of the $[Gd(TPAC)_3\cdot H_2O]_n$ (**2**) complex. Because there is a large energy gap (ca. 32000 cm^{-1}) between the $^8S_{7/2}$ ground state and the first $^6P_{7/2}$ excited state of the Gd^{3+} ion, it cannot accept any energy from the first excited triplet state of the ligand via intramolecular ligand-to-metal energy transfer. Thus the phosphorescence spectra of complex **2** actually reveals the triplet energy level ($^3\pi\pi^*$) of HTPAC in the Tb^{3+} complexes. The excitation spectrum of the complex **2** exhibits a broad band between 250 and 450 nm (Figure S4, Supporting Information), with a maximum around 330 nm which may be attributed to the ligand-centered $S_0\rightarrow S_1$ (π,π^*) transition of the thiophene moiety. The phosphorescence spectrum of the complex **2** (Figure S5, Information) also displays a broad band between 350 and 650 nm with a maximum around 550 nm when excited in the $S_0\rightarrow S_1$ transition (330 nm). On the basis of the phosphorescence spectra of complex **2**, the triplet energy level of HTPAC corresponds to the lower emission edge wavelength and appear at 22321 cm^{-1} (448 nm). The singlet energy level ($^1\pi\pi^*$) of HTPAC can be estimated by referencing its higher absorption edge, which appear at 31250 cm^{-1} (320 nm). It is interesting to note that the triplet energy level of HTPAC is above the energy of the main emitting level of $^5D_4$ of Tb^{3+}, indicating that the HTPAC ligand can act as an antenna to photosensitize the Tb^{3+} ion.

The normalized excitation spectra for the Tb^{3+} complexes, which were recorded at 303 K, and monitored around the intense $^5D_4\rightarrow{}^7F_5$ transition of the Tb^{3+} ion, are shown in Figure 4. The excitation spectra for all three complexes exhibit a broad band between 250 and 450 nm, which is attributable to the ligand centered $S_0\rightarrow S_1$ (π,π^*) transition of the aromatic thiophene moiety.[23] The excitation spectrum of **1** also exhibits a series of sharp bands arising from 4f–4f transitions from the ground state $^7F_5$ level to the $^5L_6$ (341), $^5L_9$ (351), $^5L_{10}$ (369), $^5G_6$ (378), $^5D_3$ (380) and $^5D_4$ (488) excited. However, these transitions are less intense than that of the broad band attributable to the ligand levels, which proves that luminescence sensitization via ligand excitation, is more efficient than the direct excitation of the Tb^{3+} ion absorption levels. Interestingly, in the excitation spectra of complexes **3** and **4** the intensity of the absorption band at 340 nm due to the $^7F_5\rightarrow{}^5L_6$ 4f–4f transitions (inset of Figure 4) is considerably less than that of the free ligand. Thus, the luminescence sensitization via excitation of the ligand is more effective than direct excitation of the Tb^{3+} ion in these particular complexes.

The emission spectra of the complexes **1**, **3** and **4** (λ_{ex} = 290, 330 and 330 nm, respectively) exhibit the characteristically narrow band emissions for Tb^{3+} and correspond to the $^5D_4$–^7F_J (J = 6–3) transitions (Figure 5). The most intense emission which is centered at 545 nm, corresponds to the $^5D_4\rightarrow{}^7F_5$ transition and is responsible for the brilliant green emission color of these complexes.[12] Furthermore, the fact that the ligand emission in the region 250–450 nm could not be detected in the emission spectra of these complexes indicates that efficient energy transfer between the ligand excited states and the emissive level of the Tb^{3+} ion.

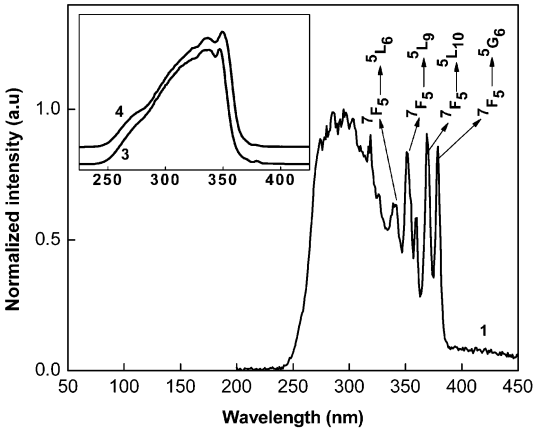

Figure 4. Room-temperature excitation spectra of complexes **1**, **3** and **4**.

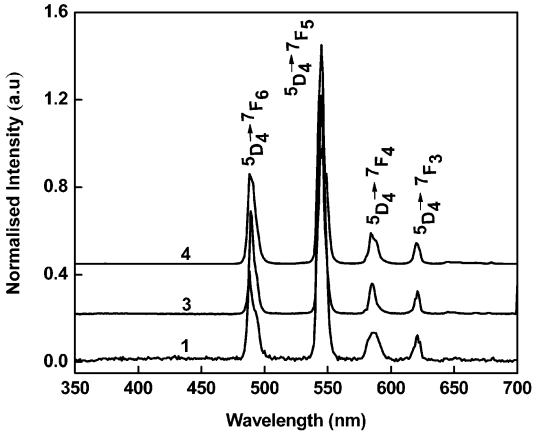

Figure 5. Room-temperature emission spectra of complexes **1**, **3** and **4**.

The overall quantum yield ($\Phi_{overall}$) for a lanthanide complex treats the system as a "black box" in which the internal process is not considered explicitly. Given that the complex absorbs a photon (i.e. the antenna is excited), the overall quantum yield can be defined as shown.[26] $\Phi_{transfer}$ is the efficiency of energy transfer from the ligand to Tb^{3+} and Φ_{Tb}, represents the intrinsic quantum yield for the lanthanide cation. The overall quantum yields ($\Phi_{overall}$) for **1**, **3** and **4** were found to be 0.07 ± 0.01, 4.43 ± 0.44 and 9.06 ± 0.90%, respectively.

$$\Phi_{overall} = \Phi_{transfer}\Phi_{Tb}$$

It is clear that **1**, which has water molecules in the one-dimensional coordination sphere exhibits a lower quantum yield. This is due to the presence of O–H oscillators in this system, which effectively quenches the luminescence of the Tb^{3+} cation. Furthermore, the energy transfer between the lanthanide ions themselves is a nonradiative process and would account for the decrease in the terbium cation emission intensity, particularly when the metal ion concentration is high.[27] In contrast, **3** and **4** exhibit high quantum yields due to the displacement of solvent molecules from the coordination sphere by the bidentate nitrogen donor ligands. Additionally, the bidentate nitrogen donor present in the coordination sphere of these complexes may also cause energy transfer to the neighboring HTPAC ligand. Following this, the HTPAC ligand subsequently transfers energy to the Tb^{3+} cation via the usual triplet pathway thus explaining the increased luminescence intensity in the present study. Of **3** and **4**, the latter exhibits a particularly high quantum yield due to the extended conjugation induced by the introduction of two phenyl groups in the 4- and 7-positions of the phenanthroline ligand.

The $^5D_4$ lifetime values ($\tau_{obsd.}$) were determined from the luminescent decay profiles for **1**, **3** and **4** at room temperature by fitting the data with a monoexponential curve. This analysis indicated the presence of single chemical environment around the emitting Tb^{3+} cation. Typical decay profiles for **1** and **4** are shown in Figure 6. The somewhat shorter lifetime observed for complex **1** than for complexes **3** and **4** ($\tau = 1.05 \pm 0.01$ ms for **1**; 1.35 ± 0.01 ms and 1.73 ± 0.01 ms for **4**) may be due to the dominant nonradiative decay channels associated with vibronic coupling due to the presence of water molecules, as has been well documented in the case of several hydrated terbium complexes. On the other hand, longer lifetime values were observed for complexes **3** and **4** due to the absence of nonradiative decay pathways. The observed quantum yields and lifetime values, especially those for **4**, are promising when compared with the recently reported 5-(thiophen-3-yl)isophthalate–terbium complex (Φ = 7.46% and τ = 213.9 μs in aqueous solution),[22] terbium-thiophenyl-derivatized nitrobenzoate complexes (Φ = 4.7–9.8% and τ = 208–725 μs in methanol solution)[21] and the terbium complex of thiophenecarboxylic acid (τ = 230 μs in solid state).[14]

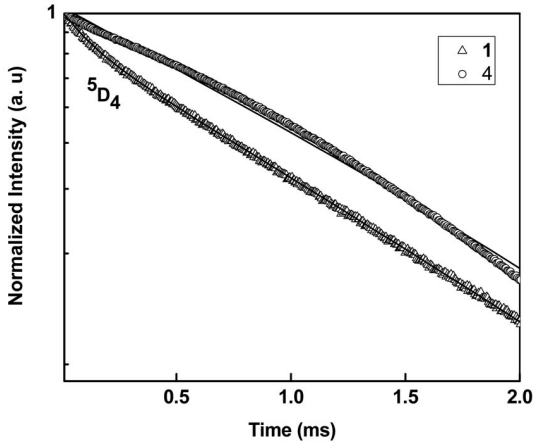

Figure 6. Experimental luminescence decay profiles of complexes **1** and **4** monitored around 545 nm and excited at their maximum emission wave lengths.

Energy Transfer Between Ligands and Terbium(III)

In general, the sensitization pathway in luminescent terbium complexes consists of excitation of the coordinated ligands into their excited states, subsequent intersystem crossing of the ligands to their triplet states, and energy

transfer from the triplet state of the ligand to the ^5D_J manifold of the Tb^{3+} cation. This is followed by internal conversion to the emitting $^5D_4$ state, and finally the Tb^{3+} cation emits radiation. Therefore, the energy level match between the triplet states of the ligands to the $^5D_4$ state of the Tb^{3+} cation is one of the key factors which governs the luminescence properties of terbium complexes. It is well known that in organolanthanide complexes neutral ligands often play a role in terms of absorbing and transporting energy to other ligands or to the central metal ion.[28] It is clear from Figures 7 and 8 that there is a large area of overlap between the room-temperature emission spectrum of the bidentate nitrogen donor and the phosphorescence spectrum of $[Gd(TPAC)_3{\cdot}H_2O]_n$ and hence any secondary ligand present in the coordination sphere of the **3** and **4** can efficiently transfer its absorbed energy to the triplet state of the HTPAC. Furthermore, the bidentate nitrogen donor ligand can also transfer energy to itself and thus undergo singlet-triplet excitation. A schematic energy level diagram based on the foregoing is presented in Figure 9.

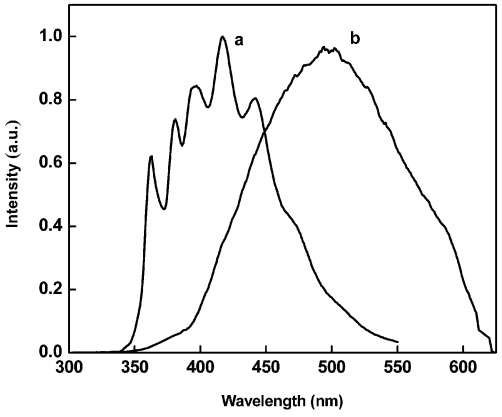

Figure 7. Emission spectra of phen (solid state) 303 K (a); and emission spectra of $[Gd(TPAC)_3{\cdot}H_2O]_n$ at 77 K ($CDCl_3$ solution, b).

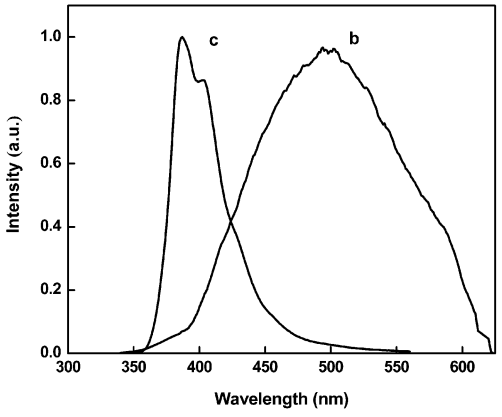

Figure 8. Emission spectra of bath (solid state) 303 K (c); and emission spectra of $[Gd(TPAC)_3{\cdot}H_2O]_n$ at 77 K ($CDCl_3$ solution, b).

In order to elucidate the energy transfer process, the phosphorescence spectra of the complexes $[Gd(TPAC)_3{\cdot}H_2O]_n$ (Figure S4, Supporting Information) and $Gd(bath)_2(NO_3)_3$ (Figure S6, Supporting Information) were measured for the triplet energy levels of the ligands. On the basis of the phosphorescence spectra, the triplet energy levels of $[Gd(TPAC)_3{\cdot}H_2O]_n$ and $Gd(bath)_2(NO_3)_3$, correspond to their lower emission edge wavelengths and appear at 22321 cm^{-1} (448 nm) and 21000 cm^{-1} (476 nm), respectively. The singlet energy levels ($^1\pi\pi^*$) of HTPAC and bath can be estimated by referencing their higher absorption edges, which appear at 31250 cm^{-1} (320 nm) and 29000 cm^{-1} (344 nm), respectively. The singlet and triplet energy levels for phen (31000 and 22100 cm^{-1}) were taken from the literature.[29] According to Reinhoudt's empirical rule,[30] the intersystem crossing process becomes effective when $\Delta E(^1\pi\pi^* - {}^3\pi\pi^*)$ is at least 5000 cm^{-1}. The energy gaps $\Delta E(^1\pi\pi^* - {}^3\pi\pi^*)$ for HTPAC, phen, bath are 8929, 8900 and 8000 cm^{-1}, respectively. Thus, the intersystem crossing processes are effective for all of the ligands. Latva's empirical rule[31] states that an optimal ligand-to-metal energy transfer process for Ln^{3+} needs ΔE ($^3\pi\pi^* - {}^5D_J$) = 2500–4500 cm^{-1} for Tb^{3+}. The energy gaps, ΔE ($^3\pi\pi^* - {}^5D_4$) are found to be 1821, 1500 and 500 cm^{-1} for HTPAC, phen and bath, respectively. Thus these energy gap values clearly indicate that a ligand-to-metal energy transfer process is effective in these systems. However, due to narrow energy gaps between $^3\pi\pi^*$ and the ^5D_J energy level of the Tb^{3+} ion, back transfer of energy may also take place.

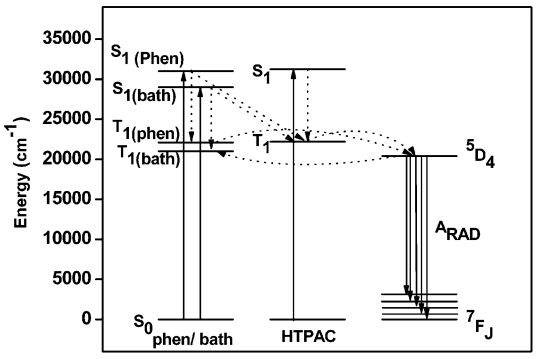

Figure 9. Schematic energy-level diagrams and energy-transfer processes for complexes **3** and **4**. S_1 represents the first excited singlet state and T_1 represents the first excited triplet state.

Conclusions

Three new complexes of Tb^{3+} with 2-thiopheneacetic acid, and in which 1,10-phenanthroline or bathophenanthroline serve as co-ligands have been synthesized and investigated on the basis of their photophysical properties. The Tb^{3+} complex **1** crystallizes in the orthorhombic space group *Pnma* with a = 7.835(10) Å, b = 19.378(10) Å, c = 13.539(10) Å, $\alpha = \beta = \gamma = 90°$ and V = 2055.6(3) $Å^3$. The unit cell contains only one crystallographically independent site for Tb^{3+} cations, contrary to those of previously reported Ce^{3+}, Pr^{3+}, Nd^{3+} and Eu^{3+} thiopheneacetate coordination polymers. Relatively short Tb–Tb distances are evident in **1** which features a triply coordinated carboxylate as

a bridging-bidentate ligand. Weak luminescence has been detected for the Tb^{3+} coordinated polymer due to the presence of a water molecule in the coordination sphere. This could also be due to the transfer of energy between the Ln^{3+} ions themselves which is a nonradiative process that becomes significant at high lanthanide concentrations. In the presence of bidentate nitrogen donor co-ligands, thermally stable binuclear complexes of the type $[Tb(TPAC)_3(phen)]_2$ or $[Tb(TPAC)_3(bath)]_2$ were produced. The overall quantum yields of these complexes were significantly enhanced by the displacement of coordinated water molecules from the coordination sphere of the thiopheneacetatoterbium complex by a highly conjugated bidentate nitrogen donor. Another factor contributing to the enhanced quantum yields might be the effective energy transfer of the secondary ligand to the triplet state of the primary ligand due to overlap of the singlet and triplet levels of the bidentate nitrogen ligand and primary ligand. Moreover, the observed quantum yields and lifetime values, especially those for **3** and **4**, were found to be promising when compared with those reported recently for a terbium 5-(thiophen-3-yl)-isophthalate complex (Φ = 7.46% and τ = 213.9 μs in aqueous solution),[22] a terbium-thiophenyl-derivatized nitrobenzoate complexes (Φ = 4.7–9.8% and τ = 208–725 μs in methanol solution)[21] and a terbium complex of thiophene carboxylic acid (τ = 230 μs in solid state).[14] However, the luminescent efficiencies observed in the present systems are found to be inferior to the *p*-aminobenzoate complexes of Tb^{3+} in the presence of bidentate nitrogen donor (Φ = 90%).[16]

Experimental Section

Materials and Methods: The commercially available chemicals terbium(III) nitrate hexahydrate, 99.9% (Acros Organics); gadolinium(III) nitrate, 99.9% (Acros Organics); 2-thiopheneacetic acid, 98% (Aldrich); 1,10-phenanthroline monohydrate, 99.5% (Merck); 4,7-diphenyl-1,10-phenanthroline, 97% (Aldrich); were used without further purification. All the other chemicals used were of analytical reagent grade.

Elemental analyses were performed with a Perkin–Elmer Series 2 Elemental Analyser 2400. A Nicolet FT-IR 560 Magna Spectrometer using KBr (neat), was used to obtain the IR spectroscopic data. Thermogravimetric analyses were carried out using a TGA-50H instrument (Shimadzu, Japan). The diffuse reflectance spectra of the new lanthanide complexes and the standard phosphor were recorded with a Shimadzu, UV-2450 UV/Vis spectrophotometer using $BaSO_4$ as a reference. The absorbance of the ligands and the corresponding complexes were measured in DMSO solution with a UV/Vis spectrophotometer (Shimadzu, UV-2450). The photoluminescence (PL) spectra were recorded using a Spex-Fluorolog DM3000F spectrofluorometer with a double grating, 0.22-m Spex 1680 monochromators, and a 450-W Xe lamp as the excitation source (front face mode). The excitation and emission spectra of the complexes were corrected for instrumental function. The lifetime measurements were carried out at room temperature using a Spex 1934 D phosphorimeter. X-ray powder diffraction (XRD) analyses were performed with a Philips X′Pert Pro diffractometer. The XRD patterns were recorded in the 5–70° 2θ range using Ni-filtered Cu-K_α radiation.

The overall quantum yields ($\Phi_{overall}$) were measured at room temperature using the technique for powdered samples described by Bril et al.,[24a] and the following expression:

$$\Phi_{overall} = \left(\frac{1 - r_{st}}{1 - r_x}\right)\left(\frac{A_x}{A_{st}}\right)\Phi_{st}$$

where r_{st} and r_x represent the diffuse reflectance (with respect to a fixed wavelength) of the complexes and of the standard phosphor, respectively, and Φ_{st} is the quantum yield of the standard phosphor. The terms A_x and A_{st} represent the areas under the complex and the standard emission spectra, respectively. In order to acquire absolute intensity values $BaSO_4$ was used as a reflecting standard. The standard phosphor used was sodium salicylate (Merck), the emission spectrum of which comprises an intense broad band with a maximum at approximately 425 nm, and a constant Φ value (60%) for excitation wavelengths between 220 and 380 nm. Three measurements were carried out for each sample, and the reported $\Phi_{overall}$ values correspond to the arithmetic mean of the three values. The errors in the quantum yield values associated with this technique were estimated to be ±10%.[24]

The X-ray diffraction data were collected at 153 K with a Nonius Kappa CCD diffractometer equipped with an Oxford Cryostream low-temperature device and a graphite-monochromated Mo-K_α radiation source (λ = 0.71073 Å). Corrections were applied for Lorentz and polarization effects. All structures were solved by direct methods[25] and refined by full-matrix least-squares cycles on F^2. All non-hydrogen atoms were allowed anisotropic thermal motion, and the hydrogen atoms were placed in fixed, calculated positions using a riding model (C–H 0.96 Å). Selected crystal data and data collection and refinement parameters are listed in Table 1. Selected metrical parameters are presented in Table 2.

CCDC-665725 (for **1**) contains the supplementary crystallographic data for this paper. These data can be obtained free of charge from The Cambridge Crystallographic Data Centre via www.ccdc.cam.ac.uk/data_request/cif.

Syntheses of Complexes

$[Tb(TPAC)_3{\cdot}H_2O]_n$ (1): An ethanolic solution of $Tb(NO_3)_3{\cdot}6H_2O$ (0.5340 g, 0.5 mmol) was added to a solution of HTPAC (0.5029 g, 1.5 mmol) in ethanol in presence of NaOH (0.1414 g, 1.5 mmol). The reaction mixture was stirred for 24 h at room temperature. After one week colorless crystals of X-ray diffraction quality were obtained. $C_{18}H_{17}O_7S_3Tb$ (600.45): calcd. C 36.00, H 2.85, S 15.98; found C 36.24, H 2.79, S 15.84. IR (KBr): $\tilde{\nu}_{max}$ = 3451, 1630, 1554, 1412, 1384, 1274, 1252, 1127, 1034, 945, 700 cm^{-1}.

$[Gd(TPAC)_3{\cdot}H_2O]_n$ (2): Complex **2** was synthesized according to the procedure described for complex **1**. $C_{18}H_{17}GdO_7S_3$ (598.76): calcd. C 36.10, H 2.86, S 16.06; found C 36.42, H 2.66, S 15.84. IR (KBr): $\tilde{\nu}_{max}$ = 3412, 1607, 1557, 1486, 1426, 1381, 1281, 1105, 696 cm^{-1}.

$Tb_2(TPAC)_6(phen)_2$ (3): An ethanolic solution of $Tb(NO_3)_3{\cdot}6H_2O$ (0.5421 g, 0.25 mmol) and 1,10-phenanthroline (0.2372 g, 0.25 mmol) were added to an aqueous solution of HTPAC (0.5105 g, 0.75 mmol) in the presence of NaOH (0.1436 g, 0.75 mmol). Precipitation takes place immediately and the reaction mixture was stirred at room temperature for 10 h. The solid produced was isolated by filtration, washed with water, followed by ethanol, then dried and stored in a desiccator. $C_{60}H_{46}N_4O_{12}S_6Tb_2$ (1524.01): calcd. C 47.24, H 3.03, N 3.67, S 12.61; found C 46.92, H 2.95, N 3.78, S 12.58. IR (KBr): $\tilde{\nu}_{max}$ = 3411, 1610, 1591, 1563, 1517, 1427, 1401, 1348, 1276, 1247, 1103, 923, 848 cm^{-1}. MS: *m*/*z* = 1524.01 (M^+).

$Tb_2(TPAC)_6(bath)_2$ (4): Complex **4** was prepared using the same procedure as that described for complex **3**. $C_{84}H_{62}N_4O_{12}S_6Tb_2$ (1829.68): calcd. C 55.14, H 3.41, N 3.06, S 10.51; found C 54.83, H 3.27, N 3.01, S 10.58. IR (KBr): $\tilde{\nu}_{max}$ = 3435, 1619, 1560, 1520, 1492, 1428, 1393, 1357, 1279, 1180, 1091, 935, 853 cm^{-1}. *m/z* = 1829.96 [M^+]. Unfortunately, all efforts to grow single crystals of complexes **2**–**4** were unsuccessful.

Supporting Information (see also the footnote on the first page of this article): TGA analysis of the complexes **1**–**4** (Figure S1), XRD patterns of complexes **1**–**4** (Figure S2), UV/Vis absorption spectra of neutral donors (Figure S3), excitation spectra of the $[Gd(TPAC)_3 \cdot H_2O]_n$ at 77 K (Figure S4), phosphorescence spectra of the $[Gd(TPAC)_3 \cdot H_2O]_n$ at 77 K (Figure S5), and phosphorescence spectra of $Gd(bath)_2 \cdot (NO_3)_3$ at 77 K (Figure S6).

Acknowledgments

The authors would like to acknowledge the financial support from Council of Scientific and Industrial Research (NWP0010), New Delhi, India. The authors also wish to thank Prof. T. K. Chandrashekar, Director, National Institute for Interdisciplinary Science and Technology, Trivandrum, India, for his constant encouragement and valuable discussions. A. H. C. thanks the Robert A. Welch Foundation (F-0003) for financial support.

[1] A. de Bettencourt-Dias, *Dalton Trans.* **2007**, 2229–2241.
[2] C. Piguet, J. C. G. Bunzli, *Chem. Soc. Rev.* **2005**, *34*, 1048–1077.
[3] J. Kido, Y. Okamoto, *Chem. Rev.* **2002**, *102*, 2357–2368.
[4] D. Parker, J. A. G. Williams, *The Lanthanides and Their Interrelation with Biosystems*; M. Dekker, Inc., New York, **2003**, vol. 40, p. 233.
[5] K. Kuriki, Y. Koike, Y. Okamoto, *Chem. Rev.* **2002**, *102*, 2347–2356.
[6] E. Brunet, O. Juanes, J. C. Rodriguez-Ubis, *Curr. Chem. Biol.* **2007**, *1*, 11–39.
[7] R. C. Evans, P. Douglas, C. J. Winscom, *Coord. Chem. Rev.* **2006**, *250*, 2093–2126.
[8] J.-C. G. Bünzli, C. Piguet, *Chem. Rev.* **2002**, *102*, 1897–1928.
[9] G. F. de Sa, O. L. Malta, C. de Mello Donega, A. M. Simas, R. L. Longo, P. A. Santa-Cruz, E. F. da Silva Jr., *Coord. Chem. Rev.* **2000**, *196*, 165–195.
[10] N. Sabbatini, M. Guardigli, J. M. Lehn, *Coord. Chem. Rev.* **1993**, *123*, 201.
[11] a) L. Sun, J. Yu, G. Zheng, H. Zhang, Q. Meng, C. Peng, F. liu, Y. Yu, *Eur. J. Inorg. Chem.* **2006**, *19*, 3962–3973; b) J. Yu, L. Z. H. Zhang, Y. Zheng, H. Li, R. D. Z. Peng, Z. Li, *Inorg. Chem.* **2005**, *44*, 1611–1618; c) A. Fratini, G. Richards, E. Larder, S. Swavey, *Inorg. Chem.* **2008**, *47*, 1030–1036; d) S. V. Eliseeva, M. Ryazanov, F. Gumy, S. I. Troyanov, L. S. Lepenev, J. C. G. Bunzil, N. P. Kuzmina, *Eur. J. Inorg. Chem.* **2006**, *23*, 4809–4820.
[12] a) S. Biju, D. B. A. Raj, M. L. P. Reddy, B. M. Kariuki, *Inorg. Chem.* **2006**, *45*,10651–10660; b) R. Pavithran, N. S. S. Kumar, S. Biju, M. L. P. Reddy, S. A. Junior, R. O. Freire, *Inorg. Chem.* **2006**, *45*, 2184–2192; c) K. Binnemans, *Handbook on the Physics and Chemistry of Rare Earths*, Elsevier, Amsterdam, **2005**, ch. 225, vol. 35, pp. 107–272.
[13] a) L. Charbonniere, S. Mameri, P. Kadjane, C. P.-Iglesias, R. Ziessel, *Inorg. Chem.* **2008**, *47*, 3748–3762; b) J. Xia, B. Zhao, H.-S. Wang, W. Shi, Y. Ma, H.-B. Song, P. Cheng, D.-Z. Liao, S.-P. Yan, *Inorg. Chem.* **2007**, *46*, 3450–3458; c) R. Shyni, S. Biju, M. L. P. Reddy, A. H. Cowley, M. Findlater, *Inorg. Chem.* **2007**, *46*, 11025–11030; d) Y. Li, F. K. Zheng, X. Liu, W. Q. Zou, G. C. Guo, C. Z. Lu, J. S. Huang, *Inorg. Chem.* **2006**, *45*, 6308–6316.
[14] a) M. Eddaudi, J. Kim, J. B. Wachter, H. K. Chae, M. O' Keeffe, O. M. Yaghi, *J. Am. Chem. Soc.* **2001**, *123*, 4368–4369; b) L. Pan, M. B. Sander, X. Li, J. Huang, M. Smith, E. Bittner, B. Bockrath, J. K. Johnson, *J. Am. Chem. Soc.* **2004**, *126*, 1308–1309; c) X. Y. Chen, Y. Bretonniere, J. Pecaut, D. Imbert, J. C. G. Bunzli, M. Mazzanti, *Inorg. Chem.* **2007**, *46*, 625–637; d) E. E. S. Teotonio, M. C. F. C. Felinto, H. F. Brito, O. L. Malta, A. C. Trindade, R. Najjar, W. Strek, *Inorg. Chim. Acta* **2004**, *357*, 451–460.
[15] A. de Bettencourt-Dias, S. Viswanathan, *Dalton Trans.* **2006**, *34*, 4093–4103.
[16] T. Fiedler, M. Hilder, P. C. Junk, U. H. Kynast, M. M. Lezhnina, M. Warzala, *Eur. J. Inorg. Chem.* **2007**, *2*, 291–301.
[17] X. Li, Y. Q. Zou, B. Zheng, H. M. Hu, *Acta Crystallogr., Sect. C* **2004**, *60*, 197–199.
[18] L.-Z. Cai, W.-T. Chen, M.-S. Wang, G.-C. Guo, J.-S. Huang, *Inorg. Chem. Commun.* **2004**, *7*, 611–613.
[19] L. Y. Wang, X. J. Zheng, L. P. Jin, S. Lu, S. Z. Lu, *Chem. J. Chin. Univ.* **1999**, *20*, 1110–1114.
[20] X. Li, Z.-Yong, Y.-Q. Zou, *Eur. J. Inorg. Chem.* **2005**, *14*, 2909–2918.
[21] S. Viswanathan, A. de Bettencourt-Dias, *Inorg. Chem.* **2006**, *45*, 10138–10146.
[22] A. de Bettencourt-Dias, *Inorg. Chem.* **2005**, *44*, 2734–2741.
[23] E. E. S. Teotonio, H. F. Brito, M. C. F. C. Felinto, L. C. Thompson, V. G. Young, O. L. Malta, *J. Mol. Struct.* **2005**, *751*, 85–94.
[24] a) A. Bril, A. W. De Jager-Veenis, *J. Electrochem. Soc.* **1976**, *123*, 396–398; b) C. D. M. Donega, S. A. Junior, G. F. de Sa, *Chem. Commun.* **1996**, *11*, 1199–1200; c) L. D. Carlos, C. D. M. Donega, R. Q. Albuquerque, S. A. Junior, J. F. S. Menezes, O. L. Malta, *Mol. Phys.* **2003**, *101*, 1037–1045.
[25] G. M. Sheldrick, *SHELL-PC Version 5; 03*, Siemens Analytical X-ray Instruments. Inc., Madison, WI, USA, **1994**.
[26] a) M. Xiao, P. R. Selvin, *J. Am. Chem. Soc.* **2001**, *123*, 7067–7073; b) S. Comby, D. Imbert, C. Anne-Sophie, J. C. G. Bunzli, L. J. Charbonniere, R. F. Ziessel, *Inorg. Chem.* **2004**, *43*, 7369–7379; c) S. Quici, M. Cavazzini, G. Marzanni, G. Accorsi, N. Armaroli, B. Ventura, F. Barigelletti, *Inorg. Chem.* **2005**, *44*, 529–537.
[27] Q. Li, T. Li, J. Wu, *J. Phys. Chem. B* **2001**, *105*, 12293–12296.
[28] H. W. Roesky, M. Andruh, *Coord. Chem. Rev.* **2003**, *236*, 91–119.
[29] X. Yu, Q. J. Su, *Photochem. Photobiol. A: Chem.* **2003**, *155*, 73–78.
[30] F. J. Steemers, W. Verboom, D. N. Reinhoudt, E. B. Van der Tol, J. W. Verhoeven, *J. Am. Chem. Soc.* **1995**, *117*, 9408–9414.
[31] M. Latva, H. Takalo, V. M. Mukkala, C. Matachescu, J. C. Rodriguez-Ubis, J. Kankare, *J. Lumin.* **1997**, *75*, 149–169.

Received: May 22, 2008
Published Online: August 20, 2008

